4. Fabrication of carbon nanotubes

4.1. Effect of pretreatment and growth temperature on the nanotube growth

4.1.1. Experimental detail

In this study we varied both the pretreatment and growth temperature to study how the growth of CNTs is affected. Details of process parameters are summarized as Table 4.1.

Table 4.1: *Process parameters for various growth temperatures.*

	Pretreatment					Growth					
Sample	Temperature (^{0}C)	Pressure (torr)	Power (W)	Time (min)	Gas ratio (H_2/sccm)	Temperature (^{0}C)	Pressure (torr)	Power (W)	Time (min)	Gas ratio (H_2/CH_4)	Bias (V)
1	400	24	600	10	90	400	24	1200	10	90:1	0
2	300	24	600	10	90	300	24	1200	10	90:1	0
3	250	24	600	10	90	250	24	1200	10	90:1	0

4.1.2. Result and discussion

Figure 4.1 shows a series of SEM photographs of CNTs films obtained at different temperatures. It is clear that there is a marked change in morphology with increasing temperature. From right to left, the surface became more uniform when the temperature range from 450^{0}C to 250 ^{0}C. It appears that growth temperature does have significant effects in changing the morphology and uniformity of the CNT films.

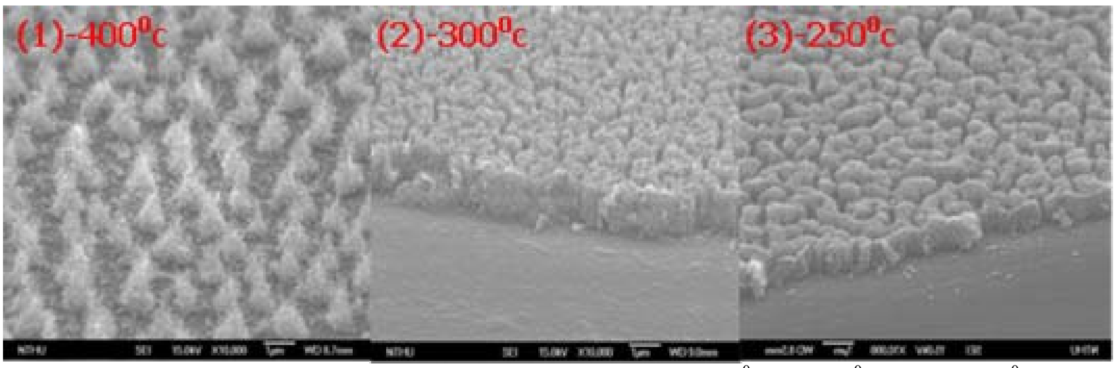

Figure 4.1: A series of SEM images of CNTs grown at (1) 400^{0}c, (2) 300^{0}c, and (3) 250^{0}c.

Figure 4.2(a) shows the corresponding Raman spectra for the three films grown at different temperatures. All spectra show that the intensity ratio of D-band and G-band (I_D/I_G) was around 1 (0.93~1.01), indicating that CNTs grown at such low temperature (250^{0}C to 450 ^{0}C) may not form complete hexagonal structures. Moreover, Figure 4.2 (b) shows that the correlation between the crystallinity (reflected in the I_D/I_G and peak position of G and D-bands) to the growth temperature is not very strong, either. Whether or not high growth temperature would actually improve the graphite crystallite has to wait for further experiments. Details information of the Raman spectra is listed in Table 4.2.

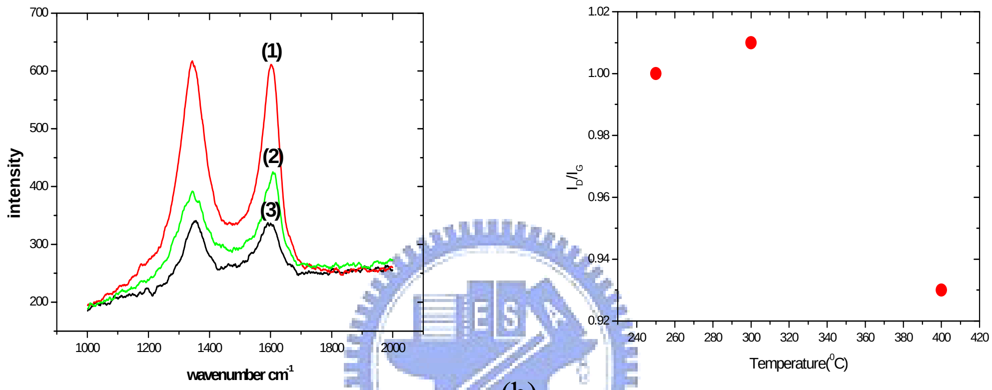

(a) (b)

Figure 4.2: (a) Raman spectra of nanotubes grown at (1) 3000c, (2) 2500c, and (3) 4000c, (b) The ID/IG dependence on growth temperature.

Table 4.2: *Characteristics of Raman spectra for various growth temperatures.*

Sample	D band(cm^{-1})	G band(cm^{-1})	I_D	I_G	I_D / I_G
1	1362	1593	353	354	1
2	1337	1606	632	623	1.01
3	1344	1611	422	455	0.93

The I-V characteristics of carbon nanotubes described above are shown in Fig. 4.3(b) and Figure 4.3(a) shows the corresponding F-N plots. Samples grown at 400^{o}C has the highest current density (0.064mA/cm^2 @V=1100V) and the lowest turn – on voltage (140V), suggesting that the difference in the electron emission properties could be due to the morphology of the films. The large separation of the 400^{o}C films is expected to reduce the “field screen effect” and results in high current density and low turn-on field. Table4.3 summarized of the field emission characteristics for the three films discussed here.

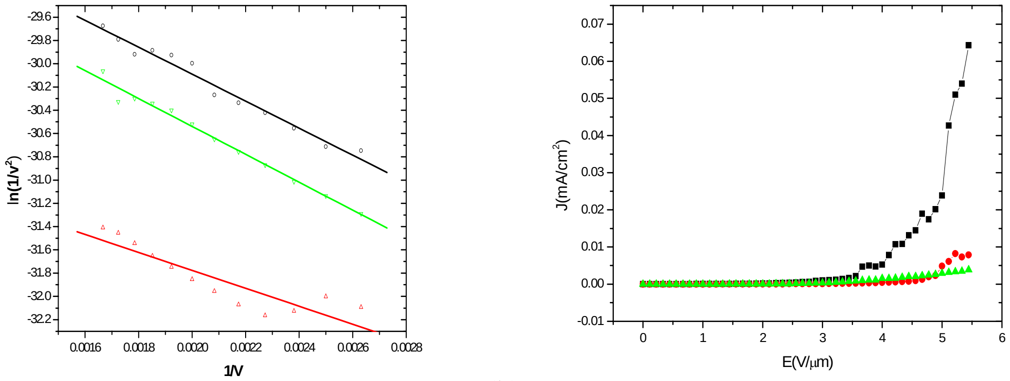

(a) (b)

Figure 4.3: (a) I-V measurement of nanotubes grown at (1) 4000c, (2) 3000c, and (3) 2500c,(b) The corresponding F-N plots of I-V curves.

Table 4.3: *Characteristic of I-V measurements for various growth temperatures.*

Sample	Turn-on field (J=0.01mA/cm^2)(V/μm)	Current density V=1100(mA/cm^2)	Field enhancement factor(β)
1	0.77	0.064	28398
2	1.33	0.007	18499
3	1.77	0.003	8931

Figure 4.4 shows the I_D/I_G dependence on the field emission properties. It is clear that there is no strong correlation between the ratio and field emission properties, including turn-on field, current density, and beta. Different growth temperature resulted in not only different graphitized structure (reflected in I_D/I_G ratio) but also the CNT distribution (observed in SEM images). We don't know that which change governs the difference in field emission performance at present.

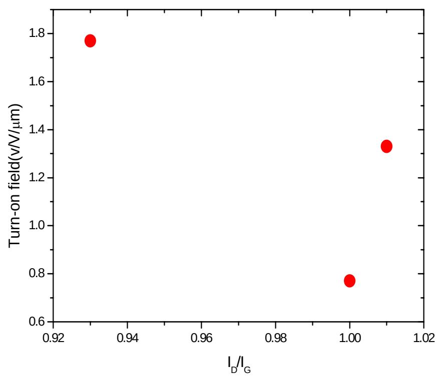

(a)

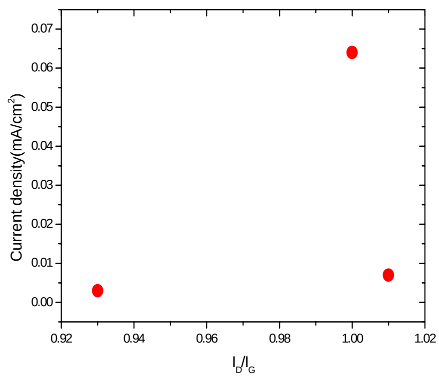

(b)

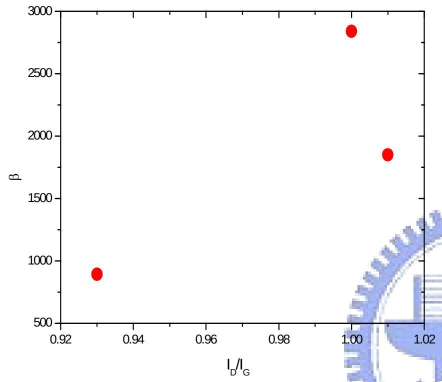

(c)

Figure 4.4: The ID/IG dependence on field emission properties; (a) Turn-on field, (b) Current density, and (c) Field enhancement factor β.

4.2. Effect of bias voltage

4.2.1. Experimental detail

In the following paragraphs we discuss the effects of applying bias voltage during growth on the structure and properties of CNTs. The detailed experimental conditions are summarized in Table 4.4. Briefly, we fixed the growth conditions at T=450 ^oC, P=24 torr, power =1200W, and H_2/CH_4=150:10, respectively, and change the bias voltage applied at substrate holder from 0~50V during growth.

Table 4.4: *Process parameters of CNT films grown under various bias voltages.*

	Pretreatment					Growth			
Sample	Temperature (^0C)	Pressure (torr)	Power (W)	Time (min)	Gas ratio (H_2/sccm)	Power (W)	Time (min)	Gas ratio (H_2/CH_4)	Bias (V)
1	450	24	600	15	150	1200	5	150:10	0
2	450	24	600	15	150	1200	5	150:10	50
3	450	24	600	15	150	1200	5	150:10	100
4	450	24	600	15	150	1200	5	150:10	150
5	450	24	600	15	150	1200	5	150:10	200

4.2.2. Results and discussion

Fig 4.5 shows a series of images for CNTs films obtained with different applied bias voltages. It is clear that applied bias voltage has some effects in improving the alignment of CNTs. In addition, all samples appear to have metal particles on the top, indicating that CNTS growth follows the tip-growth model. We note that there are some observable CNT clusters in our samples. It is not clear at present what cause the formation of these clusters. On the other hand, the applied bias does not seem to have any discernable effect on the density of CNTs, at least as far as the SEM images can tell.

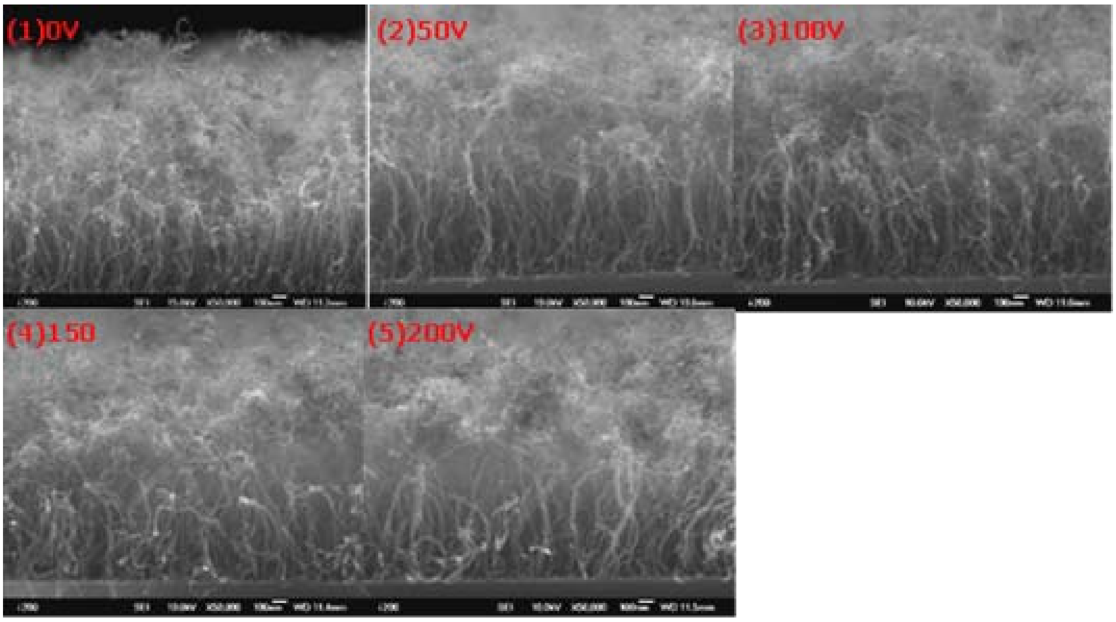

Figure 4.5: A series of SEM images of CNTs under different applied bias voltage of (1)0V, (2)50V, (3)100V, (4)150V, and (5)200V.

Figure 4.6(a) shows the Raman spectra for films grown with different applied bias voltage. In all spectra, the G-band peaks locate around 1600cm^{-1} and D-band peaks locate around 1350cm^{-1}. Unlike those observed in films grown at different temperatures where the peak position of G and D-bands is more spreaded, this series of CNT films are of more uniform bonding nature. Details of Raman spectra data were listed in Table 4.5.As is evident from Figure 4.6(b), there is an increase in the ratio of I_D/I_G with increasing applied bias voltage, indicating a certain trend is prevailing with the applied bias. Since the smaller I_D/I_G ratio means the better graphitized crystalline structure [4.1], the current results indicate that the applied bias voltage indeed improves the graphitized structure of nanotubes. Also, it is noted that the crystallite size also increases with the strength of bias voltage [4.1].

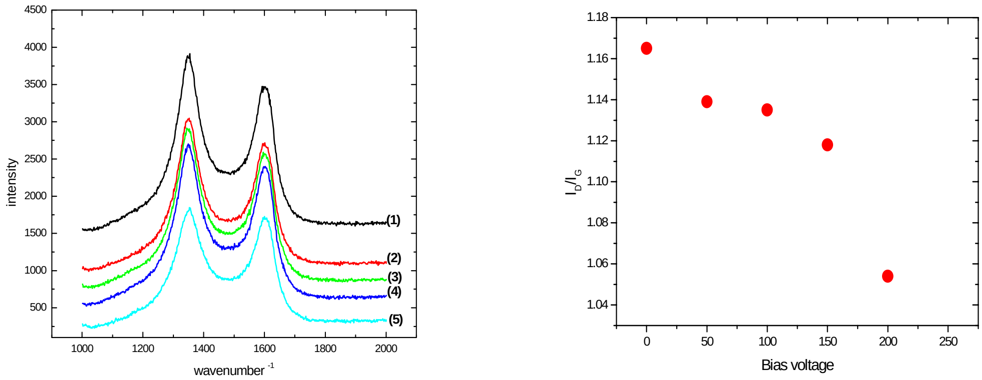

Figure 4.6: (a) Raman spectra of nanotubes as a function of applied bias voltage at (1)0V, (2)50V, (3)100V, (4)150V, and (5)200V. (b) The ID/IG dependence on bias voltage.

Table 4.5: *Characteristic of Raman spectra of CNT films grown under various bias voltages.*

Sample	D band(cm^{-1})	G band(cm^{-1})	I_D	I_G	I_D / I_G
1	1354	1592	3115	2675	1.165
2	1352	1601	2747	2417	1.139
3	1345	1596	2864	2539	1.135
4	1349	1597	2902	2595	1.118
5	1353	1600	2347	2225	1.054

Figure 4.7 shows TEM images of the as-grown CNTs. The nanotubes have diameter of 10-30 nm and length of 1-1.5 micrometer, respectively. In Figure 4.7(a), with no bias voltage applied, almost all the CNTs were nanofibers, indicating that these CNTs were not well-graphitized. On the other hand, with an applied bias voltage of 100volts (Fig. 4.7(b)) and 200volts (Fig.4.7(c)), abundance of MWNT is clearly evident. These observations may explain why the intensity ratio decreased with increased large bias voltage during growth due to the improved crystallite structure

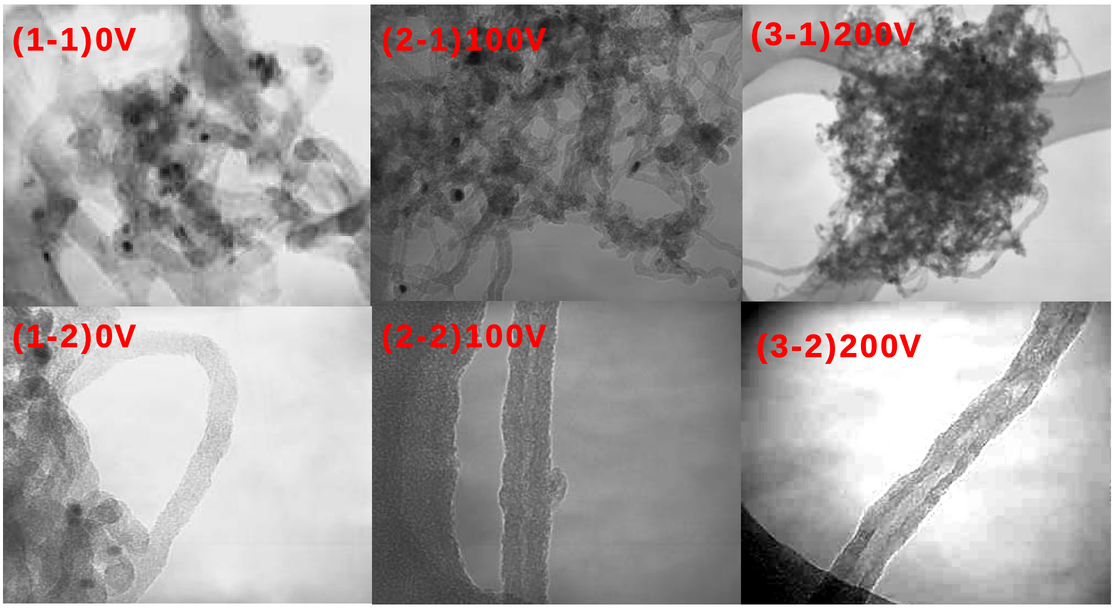

Figure 4.7: High resolution TEM images of nanotubes with different applied voltage of (1)0V, (2)100V, and (3)200V.

Figure 4.8 shows the I-V characteristics and corresponding F-N plot of CNTs grown with different bias voltages. The details of emission properties and experimental conditions are summarized in Table 4.6.

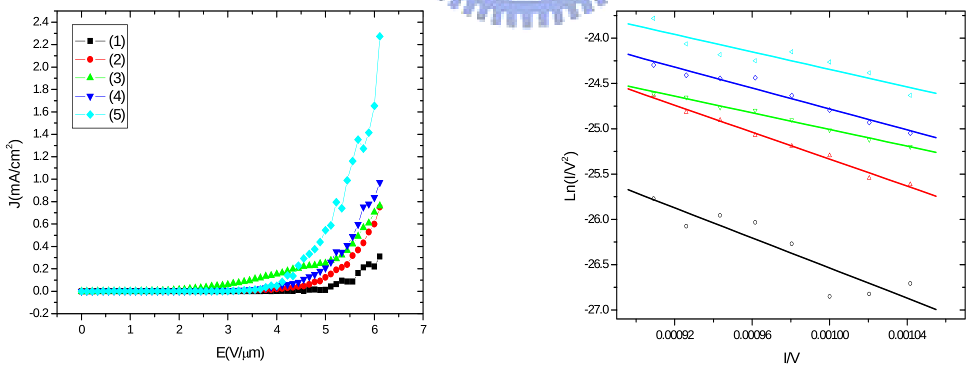

Figure 4.8: (a) I-V characteristics of nanotubes under different applied bias voltage (1)0V, (2)50V, (3)100V, (4)150V, and (5)200V, (b) The corresponding F-N plots of I-V curve.

Table 4.6: *Characteristic of I-V measurement of CNT films grown under various bias voltages.*

Sample	Turn-on field (J=0.1mA/cm^2)(V/μm)	Current density V=1100(mA/cm^2)	Field enhancement factor(β)
1	2.88	0.31	1654
2	1.11	0.75	1847
3	0.55	0.76	2991
4	1	0.97	1381
5	1.88	2.27	2884

Figure 4.9 (b) shows that the current density (@ V=1100V) increased with increasing bias voltage. Figure 4.9(c) shows that beta derived from I-V measurements slightly decreased with rising applied bias voltage. Viewed in this light, some trend in current density is prevailed with bias voltage. We were not sure whether the difference of graphite structure resulted in the improvement of current density or not

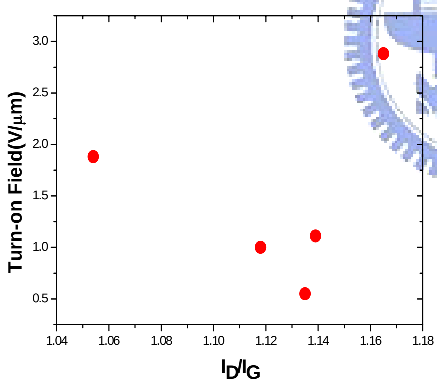

(a)

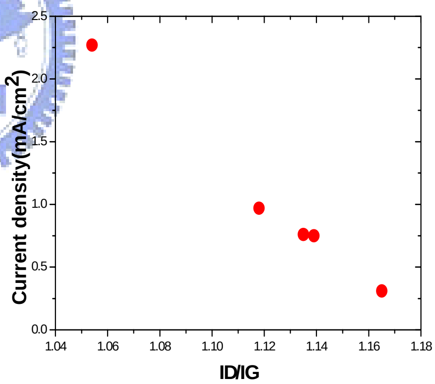

(b)

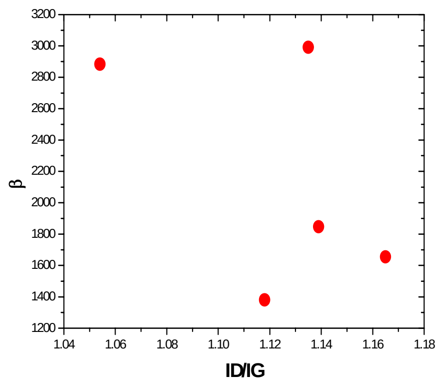

(c)

Figure 4.9: The I_D/I_G dependence on field emission properties; (a) Turn-on field, (b) Current density, and (c) Field enhancement factor β.

4.3. Effect of adding nitrogen and oxygen as assistant gases

4.3.1. Experimental detail

In this section, we study the effects of N_2 and O_2 in the growth of carbon nanotubes. CH_4 was used as the feedstock carbon source, H_2 as the plasma gas, and N_2 and O_2 as the assistant gases. In the first stage, substrate was pretreated in H_2 gas plasma for 10 min. In the second stage, a gas mixture was introduced into the chamber with a $H_2/CH_4/N_2$ flow ratio of 150:10:10~110 s.c.c.m (group A) or with a $H_2/CH_4/O_2$ flow ratio of 150:10:3~9s.c.c.m (group B). Details about the pretreatment and growth condition were collected shown as Table 4.7 and Table 4.8.

Table 4.7: *Process parameters of CNT films with various N_2.*

	Pretreament					Growth			
Sample	Temperature (^0C)	Pressure (torr)	Power (W)	Time (min)	Gas ratio (H_2/sccm)	Power (W)	Time (min)	Gas ratio ($H_2/CH_4/N_2$)	Bias (V)
1	450	24	600	15	150	1200	5	150:10:10	0
2	450	24	600	15	150	1200	5	150:10:30	0
3	450	24	600	15	150	1200	5	150:10:70	0
4	450	24	600	15	150	1200	5	150:10:90	0
5	450	24	600	15	150	1200	5	150:10:110	0

Table 4.8: *Process parameters of CNT films with various N_2*

	Pretreament					Growth			
Sample	Temperature (^0C)	Pressure (torr)	Power (W)	Time (min)	Gas ratio (H_2/sccm)	Power (W)	Time (min)	Gas ratio ($H_2/CH_4/O_2$)	Bias (V)
1	450	24	600	15	150	1200	5	150:10:3	100
2	450	24	600	15	150	1200	5	150:10:5	100
3	450	24	600	15	150	1200	5	150:10:7	100
4	450	24	600	15	150	1200	5	150:10:9	100

4.3.2. Results and discussion

Figure 4.10 shows the SEM images of CNTs as a function of different N_2 flow rate. As can be seen from Fig.4.10, the number of clusters on the top of CNTs is decreasing with the increasing N_2 flow rate. At the flow rate of $H_2/CH_4/N_2$=150:10:90, the top of CNT films is almost absent of metal clusters. Similar effect has also been observed in the oxygen-added process. Figure 4.11 shows the similar observation with O_2 process. Both processes could change the CNT films surface morphology. It seems reasonable to say that oxygen burns out with carbon atoms and reduced the support of carbon-based species, such as amorphous carbon, C_2 dimer, and C_3 trimmers. The reason for the disappearance of these clusters would be taken up in further study.

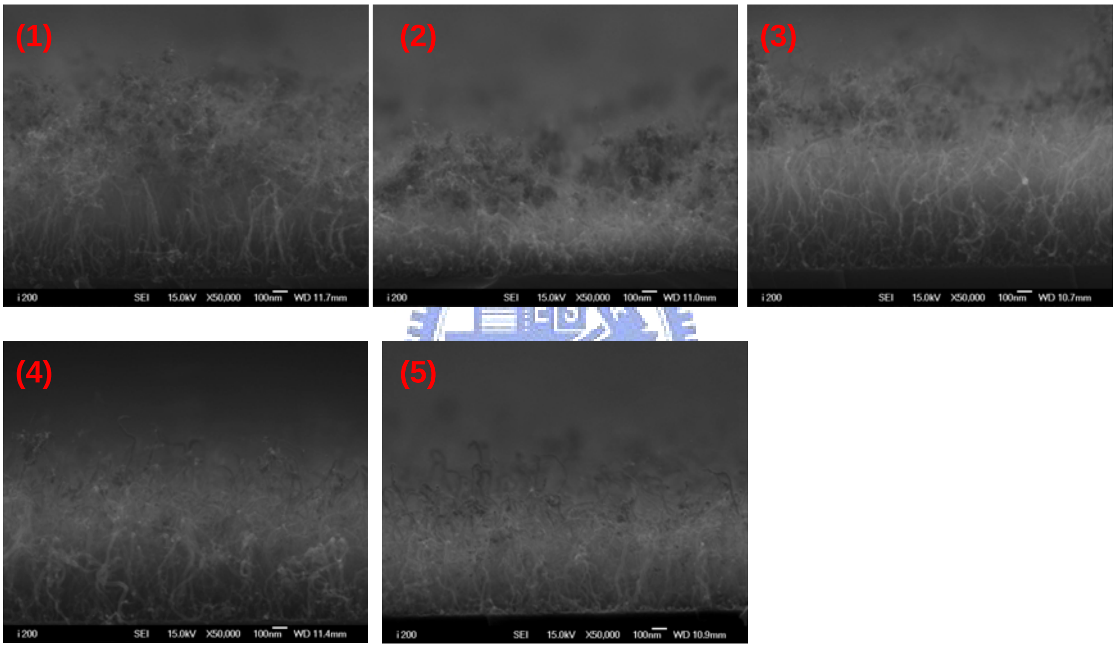

Figure 4.10: SEM images of nanotube grown with different gas flow ratio (H2:CH4:N2) (1)150:10:10, (2)150:10:30, (3)150:10:70, (4)150:10:90, (5)150:10:110[unit:s.c.c.m]

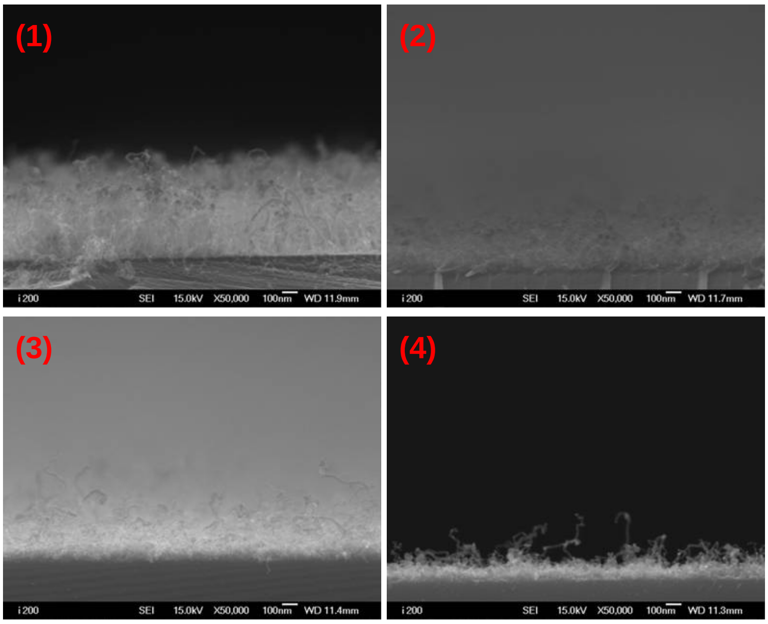

Figure 4.11: SEM images of nanotube grown with different gas flow ratio (H2:CH4:O2): (1)150:10:3, (2)150:10:5, (3)150:10:7, and (4)150:10:9. [unit:s.c.c.m].

Figure 4.12(a) and figure 4.13(a) show the Raman spectra of CNTs with N_2 and O_2 as assistant gas, respectively. Characteristics were summarized in Table 4.9 and Table 4.10. It can be revealed Figure 4.13(b) that I_D/I_G ratio reduced with addition of N_2 as assistant gas. That is, improves the crystalline quality of CNTs bodies. By contrast, figure 4.14(b) tells us that O_2 process results in poor crystalline quality.

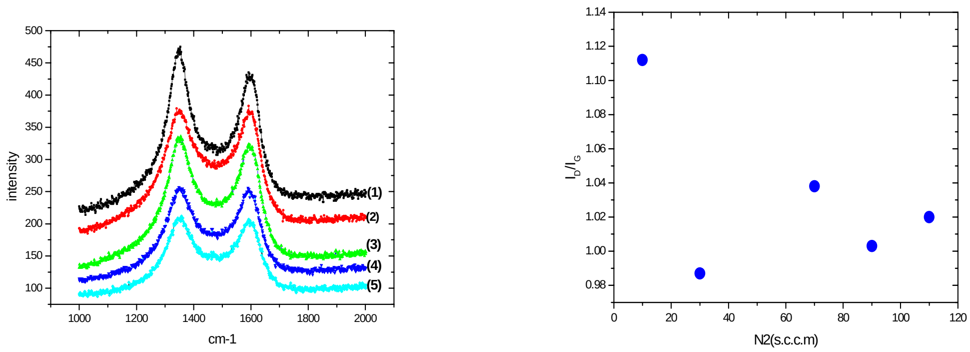

(a) (b)

Figure 4.12: (a) Raman spectra of nanotube as function of gas flow ratio (H2:CH4:N2) (1)150:10:10, (2)150:10:30, (3)150:10:50, (4)150:10:70, (5)150:10:90, (6)150:10:110[unit:s.c.c.m], (b) The ID/IG dependence on N2 flow rate.

Table 4.9: *Characteristic of Raman spectra of CNT films grown with various N_2 flow rate.*

Sample	D band(cm^{-1})	G band(cm^{-1})	I_D	I_G	I_D / I_G
1	1353	1592	395	355	1.112
2	1340	1592	329	333	0.987
3	1354	1592	326	314	1.038
4	1348	1589	257	256	1.003
5	1357	1592	252	247	1.020

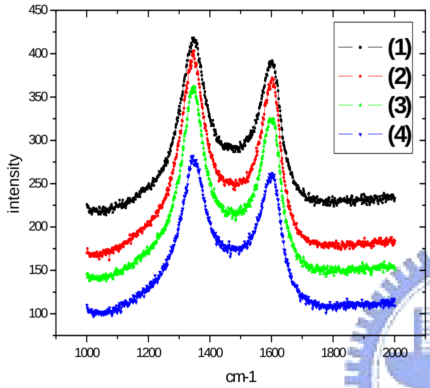

(a)

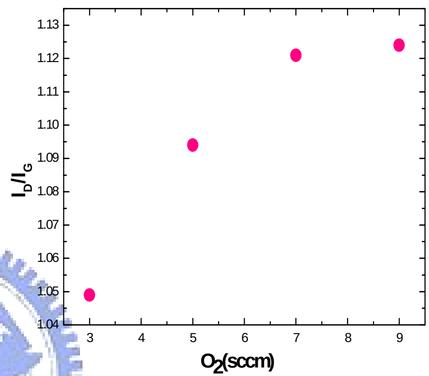

(b)

Figure 4.13: Raman spectra of nanotube as function of gas flow ratio (H2:CH4:O2) : (1)150:10:3, (2)150:10:5, (3)150:10:7, and (4)150:10:9 [unit:s.c.c.m],(b) The ID/IG dependence on O2 flow rate.

Table 4.10: *Characteristic of Raman spectra of CNT films grown with various O_2 flow rate.*

Sample	D band(cm^{-1})	G band(cm^{-1})	I_D	I_G	I_D / I_G
1	1343	1602	338	322	1.049
2	1345	1602	358	327	1.094
3	1348	1593	342	305	1.121
4	1344	1602	307	287	1.069

The results of the effect of N_2 and O_2 on the I-V measurement and F-N plots are shown in Figure 4.14. It is clear from Figure 4.14(a) addition of N_2 as assistant gas results in lower current density. On the contrast, figure 4.15(a) shows that field emission properties of all the samples with addition O_2 as assistant gas were improved. This may due to that O_2 react with amorphous carbon and flame out of CNTs bodies [7], that is, cleaning of CNTs surface, in turn, improved the characteristics of electron emission.

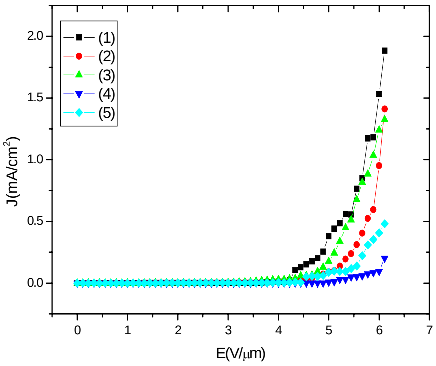

(a)

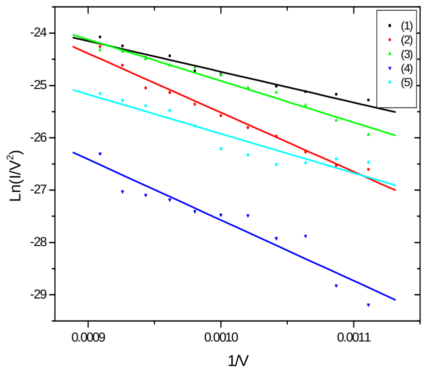

(b)

Figure 4.14: (a) I-V characteristics of nanotubes as a function of gas flow ratio: (H2:CH4:N2) (1)150:10:10, (2)150:10:30, (3)150:10:70, (4)150:10:90, (5)150:10:110 [unit:s.c.c.m], (b) The corresponding F-N plots of I-V curve.

Table 4.11: *Characteristic of I-V measurement of CNT films grown with various N_2 flow rate.*

Sample	Turn-on field (J=0.1mA/cm^2)(V/ μ m)	Current density V=1100(mA/cm^2)	Field enhancement factor(β)
1	4	1.88	2338
2	5	1.41	1216
3	4.77	1.32	1733
4	6.01	0.20	1184
5	5.33	0.48	1829

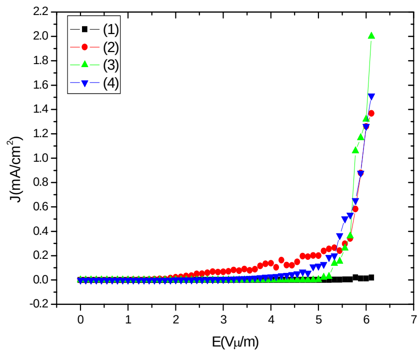

(a)

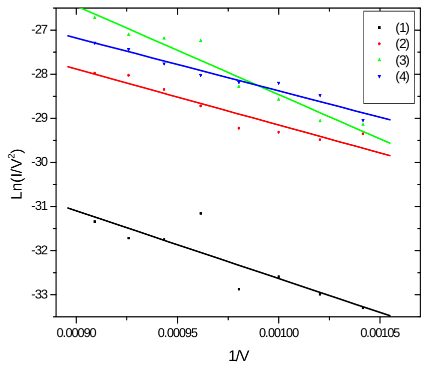

(b)

Figure 4.15: (a)I-V characteristics of nanotubes as a function of gas flow ratio (H2:CH4:O2): (1)150:10:3, (2)150:10:5, (3)150:10:7, and (4)150:10:9 [unit:s.c.c.m], (b) The corresponding F-N plots of I-V curve.

Table 4.12: *Characteristic of I-V measurement of CNT films grown with various O_2 flow rate.*

Sample	Turn-on field (J=100 μ A/cm^2)(V/ μ m)	Current density V=1100(mA/cm^2)	Field enhancement factor(β)
1	5.33	0.00098	894
2	1.22	0.0684	1084
3	6.15.11	0.1	684
4	2.55	0.075	1148

Figure 4.16 shows that there is no strong correlation between I_D/I_G and turn-on field, current density, and beta. Similar results were observed in O_2 process (obtained from figure 4.17). It is reasonable to obtain such a result. Both processes have change the surface morphology and this will have some kind influence on field emission! This is why we can not find some correlation just between I_D/I_G and field emission properties.

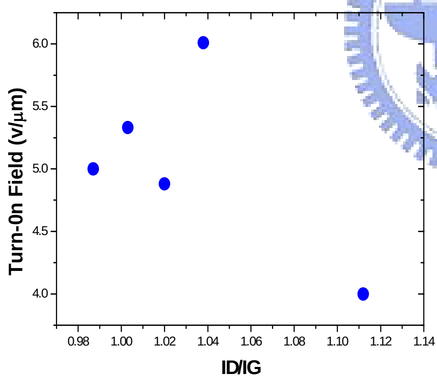

(a)

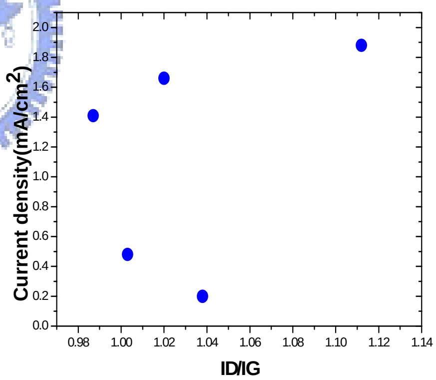

(b)

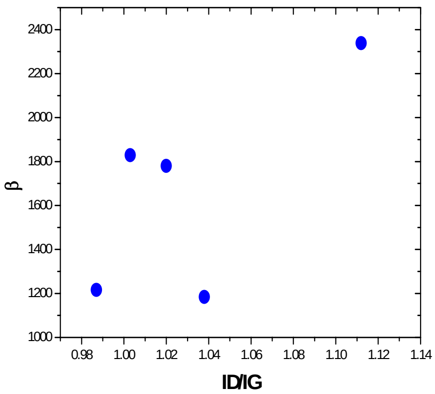

(c)_

Figure 4.16: The I_D/I_G dependence on field emission properties; (a) Turn-on field, (b) Current density, and (c) Field enhancement factor β.

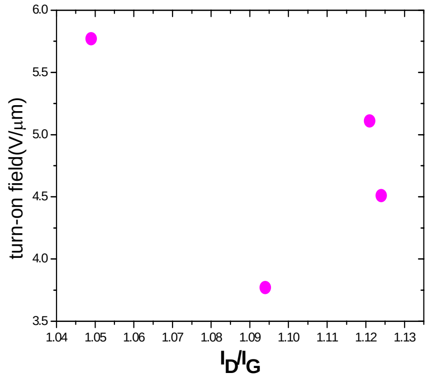

(a)

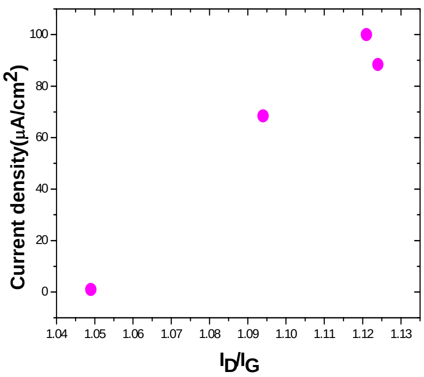

(b)

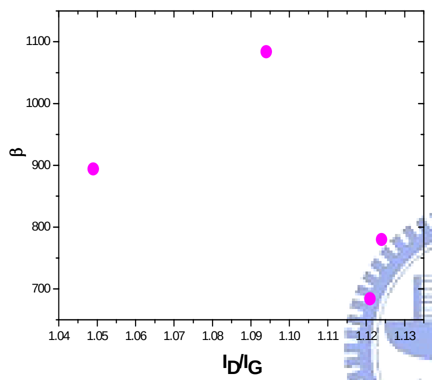

(c)

Figure 4.17: The I_D/I_G dependence on field emission properties; (a) Turn-on field, (b) Current density, and (c) Field enhancement factor β

4.4. The effect of morphology on field emission property

We suggest that morphology of CNT films have significant influence on field emission properties. Figure 4.18 shows the CNTs images grown at different condition but with the same I_D/I_G ratio. It is clear that these CNTs have absolutely different morphology. Figure 4.18(c) shows the corresponding IV-measurements of these CNT films. CNT film with large separation distance has the better emission property, even though both CNT film have the same I_D/I_G ratio.

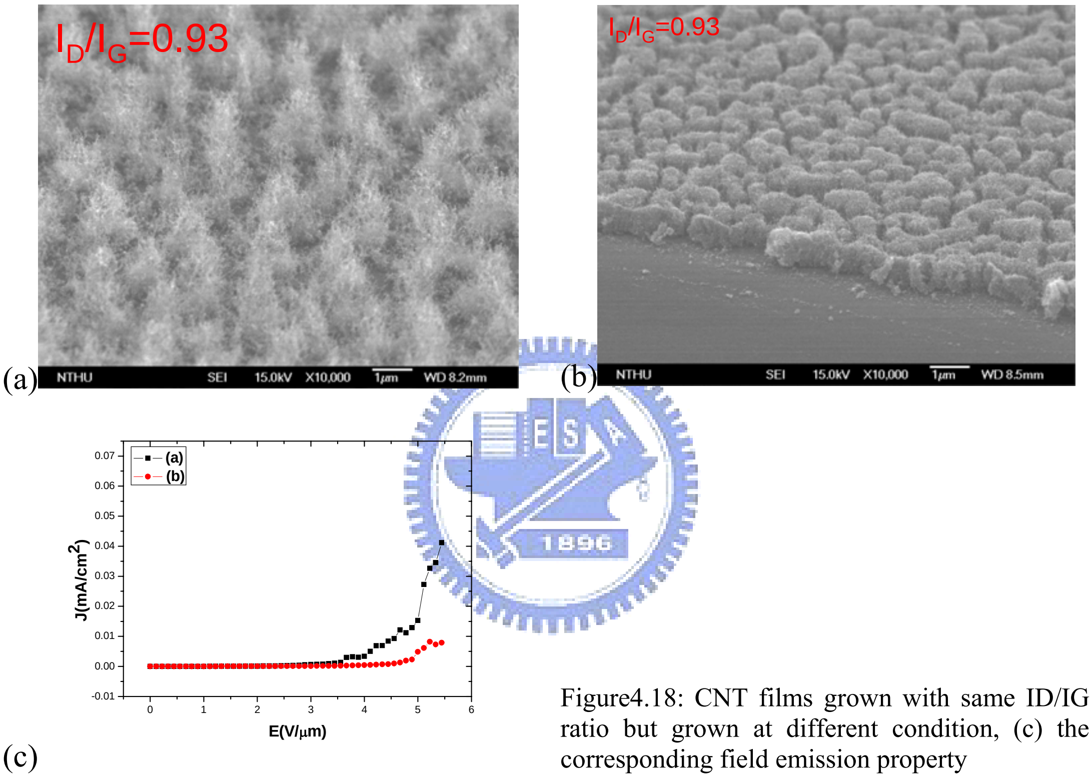

Figure4.18: CNT films grown with same ID/IG ratio but grown at different condition, (c) the corresponding field emission property

4.5. Conclusion

Many modifications of growth condition parameters have been investigated in this section. First, applying bias voltage and addition of N_2 and O_2 were confirmed to be viable methods to modify the ratio of I_D/I_G. On the other hand, it is also found that these processes have significant influence on the surface morphology of CNTs.

Furthermore, the I_D/I_G does not have a strong corelation with the performance of field emission performance by changing the CNT growth parameters. By changing the growth parameters, both the CNT structure (reflected in I_D/I_G) and the morphology (observed in SEM images) of the as-grown CNT films were affected simultaneously .Making it rather difficult to soit out direct correlations between the I_D/I_G ratio and emission properties [4.7-4.10].

Reference

[4.1] F. Tuinstra and J. L. Koenig, J. Chem. Phys. **53**, 1126(1970).

[4.2] Q. Yang, C. Xiao, W. Chen, A. K. Singh, and T. Asai, Diamond and Related Materials, 12, 1482(2003).

[4.3] S. G. Wang, J. H. Wang, and Z.B. Ma, Diamond and Related Materials, 12, 2175(2003).

[4.4] N.Hayashi, S.I. Honda, F. Tsuji, Applied Surface science, 213, 393(2003).

[4.5] Y. Avigal and R.Kalish, Applied Physics Letters, 78, 2291(2001).

[4.6] S. H. Tsai, C. W. Chao, C. L. Lee, and H. C. Shih, Applied Physics Letters, 74, 3462(1999).

[4.7] S. H. Jo, Y. Tu, and Z. P. Huang, Applied Physics Letters, 82, 3520(2003).

[4.8] M. Chhowalla, K. B. Teo, C. Ducati, N. L. Rupesinghe, Journal of Applied Physics, 90, 5308(2001).

[4.9] Yan Chen and David T. Show, Applied Physics Letters, 76, 2469(2000).

[4.10] Chris Bower, Wei Zhu, and Otto Zhou, Applied Physics Letters, 77, 830(2000).